Acute toxicity of CCl4 but not of paracetamol induces a transcriptomic signature of fibrosis in precision-cut liver slices

Vatakuti, Suresh; Schoonen, Willem G E J; Elferink, Maria; Groothuis, Geny M M; Olinga, Peter

Published in:
Toxicology in Vitro

DOI:
10.1016/j.tiv.2015.03.015

Publication date:
2015

Toxicology in Vitro 29 (2015) 1012–1020

Contents lists available at ScienceDirect

Toxicology in Vitro

journal homepage: www.elsevier.com/locate/toxinvit

Acute toxicity of CCl_4 but not of paracetamol induces a transcriptomic signature of fibrosis in precision-cut liver slices

Suresh Vatakuti [a], Willem G.E.J. Schoonen [c], Marieke L.G. Elferink [a], Geny M.M. Groothuis [a], Peter Olinga [b,*]

[a] Division of Pharmacokinetics, Toxicology and Targeting, Department of Pharmacy, Groningen Research Institute for Pharmacy, University of Groningen, Groningen, The Netherlands
[b] Division of Pharmaceutical Technology and Biopharmacy, Department of Pharmacy, Groningen Research Institute for Pharmacy, University of Groningen, Groningen, The Netherlands
[c] Toxicology Consultant, Oss, The Netherlands

ARTICLE INFO

Article history:
Received 26 November 2014
Accepted 18 March 2015
Available online 6 April 2015

Keywords:
Prediction of fibrosis
Precision cut liver slices
Paracetamol
CCl_4

ABSTRACT

In rat *in vivo*, both paracetamol (APAP) and carbon tetrachloride (CCl_4) induce liver necrosis, but long-term treatment with CCl_4, in contrast to paracetamol, causes liver fibrosis. The aim of this study was to perform transcriptomic analysis to compare the early changes in mRNA expression profiles induced by APAP and CCl_4 in the rat precision-cut liver slice model (PCLS) and to identify early markers that could predict fibrosis-inducing potential.

Microarray data of rat PCLS exposed to APAP and CCl_4 was generated using a toxic dose based on decrease in ATP levels. Toxicity pathway analysis using a custom made fibrosis-related gene list showed fibrosis as one of the predominant toxic endpoints in CCl_4-treated, but not in APAP-treated PCLS. Moreover, genes which have a role in fibrosis such as alpha-B crystallin, jun proto-oncogene, mitogen-activated protein kinase 6, serpin peptidase inhibitor and also the transcription factor Kruppel-like-factor-6 were up-regulated by CCl_4, but not by APAP. Predicted activation or inhibition of several upstream regulators due to CCl_4 is in accordance with their role in fibrosis.

In conclusion, transcriptomic analysis of PCLS successfully identified the fibrotic potential of CCl_4 as opposed to APAP. The application of PCLS as an *ex vivo* model to identify early biomarkers to predict the fibrogenic potential of toxic compounds should be further explored.

1. Introduction

Paracetamol (APAP) and carbon tetrachloride (CCl_4) are two well-known model hepatotoxins. The mechanism of liver toxicity for both compounds is a multicellular phenomenon (Laskin et al., 1995; Rivera et al., 2001). Chronic exposure to CCl_4 *in vivo* leads to necrosis and subsequently to fibrosis. In contrast, APAP induces necrosis but no fibrosis (Rowden et al., 2006). It remains to be established why CCl_4 induces fibrosis and APAP does not. The elucidation of this difference could lead to more insight into the mechanisms of fibrosis and may also be used to find new early biomarkers for fibrosis. If such differences in the mechanism of injury between APAP and CCl_4 could be mimicked *in vitro*, this would enable the study of these processes in man by using human tissue. This would allow prediction of fibrogenic effects in man, thereby circumventing the issue of possible species differences, which arise when using animal models.

The study of fibrosis *in vitro* requires a model with an intact liver architecture that can mimic the multicellular mechanism of this process. One such model is precision-cut liver slices (PCLS), as it has all the different liver cell types in their original architecture. This PCLS model system has been validated extensively for over a decade (de Graaf et al., 2010; Ekins, 1996; Elferink et al., 2008; van de Bovenkamp et al., 2005; Westra et al., 2014a). Although the process of fibrosis *in vivo* is considered to be the

Abbreviations: ACOX1, peroxisomal acyl-coenzyme A oxidase 1; AKT1, protein kinase B alpha; APAP, acetaminophen/paracetamol; BRCA1, breast cancer 1, early onset; CCl_4, carbon tetrachloride; EDN1, endothelin-1; FGF2, fibroblast growth factor; HSC, hepatic stellate cell; HNF1A, hepatocyte nuclear factor 1 homeobox A; HNF4A, hepatocyte nuclear factor 4 alpha; IL1A, interleukin-1 alpha; LPS, lipopolysaccharide; NUPR1, nuclear protein 1; PCLS, precision-cut liver slices; PKD1, polycystin-1; PPARA, peroxisome proliferator-activated receptor alpha; PPARD, peroxisome proliferator-activated receptor delta; PPARG, peroxisome proliferator-activated receptor gamma; pSmadL/C, dually phosphorylated smad; RXRA, retinoid X receptor alpha; TFAM, mitochondrial transcription factor A; TGFB1, transforming Growth Factor Beta 1; TNF, tumor necrosis factor; TP53, tumor protein p53; UW, university of Wisconsin organ preservation solution; WME, William's medium E.

* Corresponding author at: Division of Pharmaceutical Technology and Biopharmacy, Department of Pharmacy, University of Groningen, Antonius Deusinglaan 1, 9713 AV, Groningen, The Netherlands. Tel.: +31 50 363 8373.
E-mail address: p.olinga@rug.nl (P. Olinga).

http://dx.doi.org/10.1016/j.tiv.2015.03.015
0887-2333/

result of chronic exposure, it has been shown that CCl_4 treatment leads to induction of biomarkers for hepatic stellate cell activation in liver slices, as early as after 16 h of exposure, indicating that the early phase of fibrosis can be detected in this *ex vivo* system (van de Bovenkamp et al., 2005). In addition, in PCLS, the other cell types involved in fibrosis, such as hepatocytes, endothelial and Kupffer cells, remain viable and functional during culture and can be activated, as has been shown in studies using endotoxin (Elferink et al., 2004; Olinga et al., 2001) or bile acids (Clouzeau-Girard et al., 2006; Jung et al., 2007). As the validation of the rat PCLS model is greatly supported by comparison with *in vivo* data, which is largely confined to animal studies and is scarcely available for human liver, we studied the gene expression in rat PCLS after treatment with CCl_4 and APAP. Although we do not make the comparison with *in vivo* data in this paper, we know that in rats *in vivo* CCl_4 induces liver necrosis and fibrosis and that APAP does induce only necrosis. Microarray analysis of rat liver treated with CCl_4 and APAP *in vivo* and in PCLS, using a commercial gene expression *in vivo* database, showed that rat PCLS can predict the toxicity and at least part of the pathology observed *in vivo* (Elferink et al., 2008). Data of human PCLS are currently being collected and will be analyzed and published in the future.

In the present study we performed further transcriptomic analysis from the data of the above-mentioned experiments with the rat PCLS model to characterize the gene expression profiles induced by APAP and CCl_4 and to elucidate whether a gene expression pattern related to early fibrosis could be detected for CCl_4 but not for APAP. We performed a comparison analysis with respect to the regulated genes, and also analyzed upstream regulators, which could possibly be responsible for the observed gene expression changes. If prediction of long-term toxicity appears to be feasible at an early time point using PCLS, this model would contribute greatly to reducing and refining animal experimentation and to reducing costs of toxicity testing.

2. Materials and methods

Microarray data of APAP and CCl_4 from our earlier published transcriptomic study using rat PCLS was used (Elferink et al., 2008). In these experiments rat PCLS were exposed to CCl_4 (van de Bovenkamp et al., 2005) and APAP (Elferink et al., 2008). RNA was isolated and the RNA processing and hybridization was performed as described (Elferink et al., 2008; van de Bovenkamp et al., 2005). These methods are described only briefly here; see for details these two references.

2.1. Rat liver slice preparation

Rat livers from male Wistar rats (Harlan, Zeist, The Netherlands) were harvested under anesthesia with isoflurane and stored at 4 °C in University of Wisconsin organ preservation solution (UW, Dupont Critical Care, Waukegan, IL, USA) until slicing (max 15 min). Precision-cut liver slices (diameter 8 mm, thickness 250 μm) were prepared using a Krumdieck tissue slicer in ice-cold Krebs–Henseleit buffer, pH 7.4, supplemented with glucose to a final concentration of 25 mM, saturated with carbogen (95% O_2/5% CO_2). Slices were stored at 4 °C in UW until the start of the experiment (Elferink et al., 2008).

2.2. Rat liver slice experiments

Slices were pre-incubated individually in 6-well culture plates, each slice in 3.2 ml Williams Medium E with glutamax-1 (Gibco, Invitrogen, Paisley, Scotland) supplemented with 25 mM D-glucose and 50 μg/ml gentamycin (Gibco, Invitrogen) (WEGG medium) under carbogen atmosphere at 37 °C for 1 h, while gently shaken (90 times/min). After pre-incubation the slices were transferred to fresh WEGG medium. The experiments with APAP were performed in 6-well plates with 3.2 ml medium (Elferink et al., 2008), while CCl_4 slices were incubated in 25 ml Erlenmeyer flasks containing 5 ml medium (van de Bovenkamp et al., 2005). The toxic dose was selected at a 60–90% decrease in ATP levels with respect to corresponding controls. The PCLS were exposed to 2.5 mM APAP. CCl_4 was spotted in an amount of 5 μl on a filter paper, which was attached to the stopper with a needle and was situated above the liquid phase as described earlier (van de Bovenkamp et al., 2005). Since the toxic concentration of CCl_4 at 16 h already showed a relatively large ATP depletion, this 16 h time point was chosen in contrast to 24 h APAP samples. Three different livers were used for each experiment; for RNA isolation 3 slices were pooled and quickly frozen in liquid nitrogen and stored at −80 °C.

2.3. Isolation of RNA for microarray analysis

Total RNA was isolated from three combined slices from each experiment with the use of Trizol reagent (Invitrogen, Carlsbad, CA, USA). The RNA concentration and quality was determined with use of the NanoDrop (ND-1000 spectrophotometer) and the agilent technology (Agilent 2100 Bioanalyzer with Agilent RNA 6000 Nano kit). Before processing the purity of RNA was determined by measuring E260/E280 and the Agilent RNA Integrity number (RIN) (Schroeder et al., 2006). The E260/E280 values from all samples were >1.8. The RIN values were >8, with one exception: one 16 h control for CCl_4 with a RIN value of 7.8. If necessary, RNA was cleaned-up by extraction with phenol/chloroform/isoamylalcohol, followed by a second extraction with chloroform/isoamylalcohol and precipitation with ethanol and lithium chloride.

2.4. RNA processing and hybridization

Double-stranded cDNA was synthesized from 5 μg total RNA using the Custom Superscript ds cDNA synthesis kit (Invitrogen, Carlsbad, CA) and used as a template for the preparation of biotin-labeled cRNA with use of the Bioarray HighYield RNA Transcript Labeling kit (T7) (Enzo Life Sciences, Inc, Farmingdale, NY). After fragmentation at 1 μg/μl according to the manufacturer's protocol, biotin-labeled cRNA (10 μg) was hybridized at 45 °C for 16–17 h to the RGU34A array (Affymetrix, Santa Clara, CA). Following hybridization, the arrays were washed, stained with phycoerythrin-streptavidin conjugate (Molecular Probes, Eugene, OR), and the signals were amplified by staining the array with biotin-labeled anti-streptavidin antibody (Vector Laboratories, Burlingame, CA) followed by phycoerythrin-streptavidin. The arrays were laser scanned with a GeneChip Scanner 3000 (Affymetrix, Santa Clara, CA) according to the manufacturer's instructions.

2.5. Microarray data pre-processing and analysis

Normalization of the microarray data was performed by RMA normalization using MicroarrayRUS v.1.0 software (Dai et al., 2012). Control genes were removed from the rest of the analysis. Rank product analysis of the normalized data was performed using MicroarrayRUS v.1.0 software (Breitling et al., 2004). A list of differentially expressed genes was created using criteria of fold change of $\geqslant 1.5$ and multiple hypothesis adjusted p-value $\leqslant 0.05$ and used as input for pathway analysis in Ingenuity software.

2.6. Gene expression dynamics analysis

Gene Expression Dynamics Inspector (GEDI) transforms high-dimensional gene expression data into distinct two-dimensional (2D) color patterns. The graphical output of GEDI gives the visual representation of the samples. The metagene signature of each sample is represented in a grid of 26×25 tiles; each of the tiles contains genes that are highly correlated with each other. The tiles are arranged such that each tile is also correlated with the adjacent tiles. Thus, it allows a global first-level analysis of the data to observe the response due to the effect of a drug. Pattern analysis of the data was performed by GEDI software (default settings) to understand the global transcriptomic changes induced by compounds (Eichler et al., 2003).

2.7. Pathway and network analysis

Ingenuity Pathway Analysis ("http://www.ingenuity.com/products/ipa") was used to determine pathways and networks that could describe the toxicity of APAP and CCl_4. Rat liver tissue specific pathway analysis was performed.

2.8. Custom-made toxlist analysis

Custom-made toxlists were also considered for analysis along with toxlists present in the Ingenuity knowledgebase. Custom fibrosis toxlists were created based on our observation that the toxlist for hepatic fibrosis in IPA does not include all the known genes related to the fibrotic process. Custom-made toxlists for fibrosis were generated by using the information from different sources such as SABioscience fibrosis PCR chip ("http://www.sabiosciences.com/rt_pcr_product/HTML/PARN-120Z.html") and an in-house custom made chip with genes related to collagen synthesis and breakdown (Westraa, submitted for publication). SABioscience provides a custom fibrosis PCR array chip containing genes related to fibrosis. Finally a combined gene list is generated from the genes of IPA fibrosis toxlist, SABioscience and in-house custom array of collagen-metabolism related genes. IPA uses Fisher exact test to calculate statistical significance.

2.9. Upstream regulator analysis

Upstream Regulator Analysis was performed to identify the upstream regulators that may be responsible for the observed gene expression changes. IPA predicts which upstream regulators are likely to be activated or inhibited, which in turn could explain the gene expression changes observed in the dataset. IPA makes predictions on upstream regulators using a z-score algorithm (Krämer et al., 2014). The z-score value is calculated using the gene expression patterns of the genes downstream of an upstream regulator. *P*-value of overlap indicates the statistical significance of genes in the dataset that are downstream of the upstream regulator but unlike the z-score, it does not take into consideration up or down-regulation of genes in dataset. Upstream regulators with a z-score greater than 2 or smaller than -2 and *p*-value of 0.05 were considered significant and their role in fibrosis was studied.

2.10. Causal network analysis

Causal Networks are small hierarchical networks of regulators that control the expression of the regulated genes. This helps to identify novel upstream regulators, because they influence the expression either directly or indirectly via intermediate regulators (Krämer et al., 2014). Causal networks generated by IPA with an activation z-score greater than 2 or smaller than -2 and *p*-value of overlap 0.05 were considered significant and their role in fibrosis was studied.

3. Results

3.1. Gene expression dynamics analysis

The expression values of all the replicates of each group were averaged to make a representative self-organizing map of each group using GEDI (Fig. 1). The regions where gene expression patterns are different are indicated in boxes (as in A, B, C, and D). The change in color of the cells in those boxes can be interpreted as change in expression intensity of genes in those cells. The APAP control (A) group at 24 h is similar to the CCl_4 control group at 16 h (C), although there are slight differences, which may be ascribed to a difference in incubation time. Expression patterns of slices treated with each of the compounds were considerably different from their corresponding controls. Although visually small differences were noticed between the APAP treated (B) and CCl_4 treated (D) group, the gene expression intensity levels were different in those highlighted regions. Since each tile in the GEDI map contains a group of correlated genes, such minor differences could indicate the difference between compounds. Thus, GEDI analysis revealed evidence on the global level that APAP and CCl_4 have induced characteristic expression profiles, which can be explained possibly by the different mechanisms of toxicity of both compounds.

3.2. Gene selection by rank product analysis

The rank product analysis method has been showed to perform well to identify the regulated genes, particularly for datasets that have a low number of samples or a high level of noise (Breitling et al., 2004). Regulated genes were selected using a criterion of fold change of $\geqslant 1.5$ and adjusted *p*-value of $\leqslant 0.05$ using the MicroarrayRUS program. The Vennplex program (Cai et al., 2013) was used to observe the commonly up- or down-regulated or contra-regulated genes. Contra-regulated genes are those that are up-regulated in one compound and down-regulated in another compound. In total 174 genes were deregulated in the case of CCl_4 and 116 genes were deregulated in the case of APAP, while 63 genes were similarly regulated in the presence of both compounds, of which 19 genes were up-regulated and 44 genes were down-regulated. No contra-regulated genes were found as shown in Fig. 2. The list of genes that are specifically deregulated by either APAP or CCl_4, and also the genes that are regulated in common due to APAP and CCl_4 treatment are shown in Supplementary data S1.

3.3. Custom fibrosis toxlist analysis

Custom fibrosis toxlist analysis was performed using IPA with the toxlists obtained from the different sources described in the materials and methods section. Toxlists regulated with a *p*-value of $\leqslant 0.05$ were considered significant (corresponds to $-\log$ [*p* value] of 1.3). This analysis indicated that the set of genes in the fibrosis toxlist from SABioscience was significantly regulated by CCl_4 but not by APAP (Fig. 3). The other custom toxlists were not found to be significantly regulated as a whole. However, differences between the effects of CCl_4 and APAP were found for some individual genes for the other toxlists as well as for the combined fibrotic toxlist. Genes such as JUN, LITAF, MAPK6, PLAT and SERPINE1 from the SABioscience fibrotic toxlist were regulated by CCl_4.

In Table 1 the genes from the fibrosis toxlists that are specifically deregulated in CCl_4 are listed. Except for PLAT, all the genes

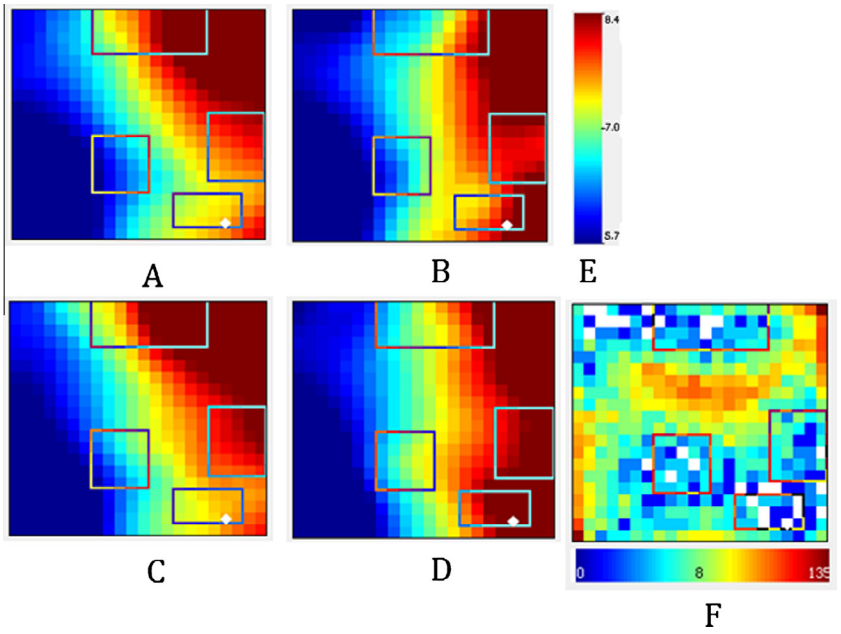

Fig. 1. Global transcriptomic changes induced by APAP and CCl_4. Comparative Gene Expression Dynamics Inspector (GEDI) analysis of averaged values of expression values from biological replicates of APAP control (A) and treated (B), CCl_4 control (C) and treated (D) samples. The Gene density map (E), indicates the number of genes in each cell (white cells indicate the absence of genes in those cells). The expression intensity is indicated in (F). Regions of difference are indicated with squares.

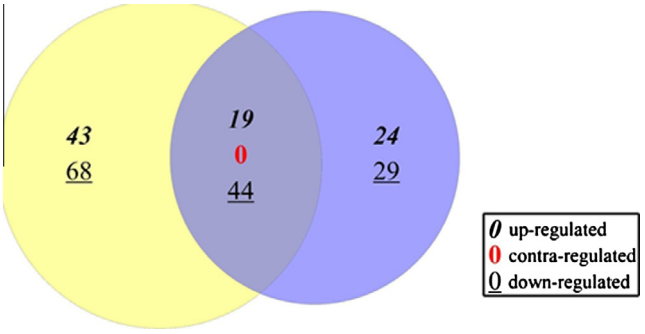

Fig. 2. Venn diagram comparison of regulated genes between APAP and CCl_4. Genes regulated with a fold change criterion of 1.5 and multiple hypothesis adjusted *p*-value of $\leqslant 0.05$ were compared. Genes regulated due to CCl_4 and APAP are indicated in yellow and blue circles respectively and the genes regulated in common are indicated in the region of interaction between yellow and blue circles. (For interpretation of the references to colour in this figure legend, the reader is referred to the web version of this article.)

mentioned in Table 1 that are known to play a role in the fibrotic process are specifically deregulated by CCl_4 and not by APAP. Furthermore, the markers specific for hepatic stellate cells such as KLF6 and CRYAB are up-regulated by CCl_4.

3.4. Upstream regulator analysis

Upstream regulator analysis revealed that several regulators are involved in controlling the expression of the genes regulated by CCl_4 and APAP treatment. These regulators and their activation z-score and p-value of overlap are shown in Tables 2 and 3 respectively. ACOX1, HNF4A and HNF1A are predicted to be inhibited and TGFB1 is predicted to be activated due to treatment with both compounds. However PKD1, AKT1, BRCA1, FGF2 and TP53 are unique to APAP treatment and PPARA, NUPR1 IL18, STAT1, TGFA, TNF, PPARD, PPARG, RXRA, TFAM, EDN1, EGF, IL1A and ERN1 are unique to CCl_4 treatment.

TGFB1, a growth factor known to play an important role in hepatic fibrosis during hepatic stellate cell activation, is predicted to be activated due to both APAP and CCl_4. However, 28 genes regulated by CCl_4 treatment are causally linked to activation of TGFB1, whereas only 19 genes are causally linked due to APAP treatment, resulting in a much lower *p* value for CCl_4 than for APAP. Mechanistic networks for visualizing the causal link between TGFB1 activation and their corresponding target molecules are shown in Figs. 4 and 5.

3.5. Causal network analysis

Causal network analysis reveals small hierarchical networks of interacting regulators, which explains the gene expression changes observed in the dataset. In the case of treatment with CCl_4, many of these networks involve multiple regulators combined with a master regulator. For example HNF4A interacts with HNF1A and

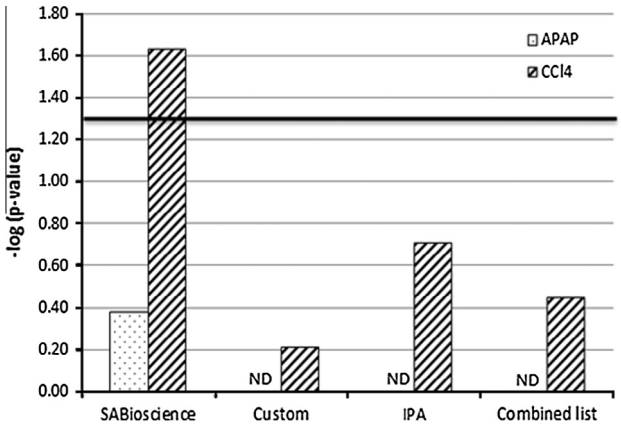

Fig. 3. Custom fibrosis toxlist analysis of APAP and CCl_4 regulated genes. Horizontal line indicates the threshold corresponding to *p*-value of $\leqslant 0.05$ and ND means that no regulated genes were found in common with the corresponding toxlist and hence overrepresentation was not assessed.

Table 1
Fibrosis related genes, which are specifically regulated in case of CCl_4. Genes known to play a role in fibrosis and are specifically regulated in CCl_4 with corresponding fold change and their role in fibrosis.

Gene	Description	Fold change	Role in fibrosis
CRYAB	Crystallin, alpha B	10.5	Induced in activated hepatic stellate cells (Takahara et al., 2006)
JUN	Jun proto-oncogene	2.6	JunD is implicated in the regulation of hepatic stellate cell (HSC) activation and liver fibrosis (Kluwe et al., 2010; Smart et al., 2006).
KLF6	Kruppel-like factor 6	11	Induced in response to early fibrosis (Ratziu et al., 1998)
LITAF	Lipopolysaccharide-induced TNF factor	2.5	Induced in hepatic stellate cells (Ceccarelli et al., 2014)
MAPK6	Mitogen-activated protein kinase 6	2.5	MAPK pathway is known to be involved in the activation of HSC (Guo et al., 2009)
PLAT[a]	Tissue plasminogen activator	2	PLAT increases extra cellular matrix (ECM) degradation (Ghosh and Vaughan, 2012; Hsiao et al., 2008)
SERPINE1	Serpin peptidase inhibitor	3.7	Progression of fibrosis (Ghosh and Vaughan, 2012)

[a] Also regulated in case of APAP.

Table 2
Upstream regulators predicted to be activated or inhibited due to CCl_4 treatment. Upstream regulators with their corresponding molecular type, predicted activation or inhibition state, activation z-score and *p*-value of overlap.

Upstream regulator	Molecule type	Predicted activation	Activation z-score	*P*-value of overlap
EDN1	Cytokine	Activated	2.199	4.38E−03
EGF	Growth factor	Activated	2.669	1.05E−04
ERN1	Kinase	Activated	2.177	1.23E−04
IL1A	Cytokine	Activated	2.416	1.67E−02
IL1B	Cytokine	Activated	2.256	1.71E−06
NUPR1	Transcription regulator	Activated	2.828	2.11E−02
STAT1	Transcription regulator	Activated	2	5.33E−02
TGFA	Growth factor	Activated	2.395	2.53E−04
TGFB1	Growth factor	Activated	3.773	6.40E−04
TNF	Cytokine	Activated	3.549	1.00E−09
ACOX1	Enzyme	Inhibited	−2.626	1.38E−11
HNF1A	Transcription regulator	Inhibited	−2.605	4.55E−10
HNF4A	Transcription regulator	Inhibited	−2.933	7.28E−09
PPARA	Ligand-dependent nuclear receptor	Inhibited	−2.624	7.66E−22
PPARD	Ligand-dependent nuclear receptor	Inhibited	−2.639	1.28E−10
PPARG	Ligand-dependent nuclear receptor	Inhibited	−2.383	8.27E−07
RXRA	Ligand-dependent nuclear receptor	Inhibited	−2.594	6.74E−09
TFAM	Transcription regulator	Inhibited	−2	1.18E−04

CTNNB1, which in turn have causal relations with 23 genes in the network. All the significant networks which are predicted to be activated or inhibited due to both APAP and CCl_4 are reported in Supplementary data S2. There were 24 causal networks predicted as activated or inhibited in case of CCl_4 but only five such significant networks are reported in the case of APAP. Although the overall number of regulated genes affected by exposure to the toxic concentration of APAP or CCl_4 was more or less the same, there were large differences with respect to the resulting causal networks.

4. Discussion

In this study, we performed the comparative analysis of the gene expression profiles of rat PCLS induced by APAP and CCl_4, which are known to induce toxicity by different mechanisms. Comparison was performed using gene expression patterns, regulated genes, and pathway and upstream regulator analysis of regulated genes.

Pattern analysis using GEDI revealed characteristic expression patterns due to a toxic concentration of each of the compounds with respect to the corresponding control (Fig. 1). The relatively small differences between the APAP and CCl_4 induced expression patterns could be due to the different mechanisms of toxicity, including the onset of fibrosis due to CCl_4. Similarities in the changes in expression patterns may be explained by the fact that both compounds induce necrosis after short-term treatment, which was concluded previously both for CCl_4 after 16 h and for APAP after 24 h by ToxShield prediction (Elferink et al., 2008).

Comparison of the regulated genes showed that there is good overlap among the regulated genes and there is also a significant number of genes uniquely regulated due to either APAP or CCl_4 (Fig. 2). Some of those genes uniquely regulated due to CCl_4 treatment include fibrosis related genes (Table 1). With the exception of PLAT, these fibrosis related genes were not found to be regulated by treatment of rat PCLS with the necrosis-inducing compounds iproniazid and bromobenzene either (data not shown).

Bovenkamp et al. showed that in non-treated rat liver slices, the expression of hepatic stellate cell specific markers such as aB-crystallin, KLF6 and heat shock protein 47 remained constant during incubation for 24 h, indicating quiescence of HSC. In contrast, incubation with CCl_4 led to a time- and dose-dependent increase in mRNA expression of these markers. In accordance with these findings, in our microarray analysis, aB-crystallin, KLF6 and HSP47 were also up-regulated (van de Bovenkamp et al., 2005). Regulation of these hepatic stellate cell markers indicates initiation of the fibrotic processes in CCl_4 treated slices.

The growth factor TGFB1 plays a key role in fibrosis via hepatic stellate cell activation. When we focused on genes involved in the TGFB1 signaling pathway and their change in expression due to treatment with APAP or CCl_4, we found that more genes involved in the TGFB1 pathway are regulated by CCl_4 than by APAP: 19 target genes in the dataset have an expression direction consistent with activation of TGFB1 due to CCl_4 treatment (Fig. 4), in contrast only 13 target genes have an expression direction consistent with activation of TGFB1 due to APAP treatment (Fig. 5). This observation gives an indication of early fibrotic processes activated within 16 h due to a toxic concentration of CCl_4. From the TGFB1 network

Table 3
Upstream regulators predicted to be activated or inhibited due to APAP treatment. Upstream regulators with their corresponding molecular type, predicted activation or inhibition state, activation z-score and *p*-value of overlap.

Upstream regulator	Molecule type	Predicted activation	Activation z-score	*p*-value of overlap
AKT1	Kinase	Activated	2.207	4.77E−03
BRCA1	Transcription regulator	Activated	2.402	2.67E−04
FGF2	Growth factor	Activated	2.213	4.45E−02
TGFB1	Growth factor	Activated	2.175	1.27E−03
TP53	Transcription regulator	Activated	2.002	1.32E−02
ACOX1	Enzyme	Inhibited	−2.646	1.80E−04
HNF1A	Transcription regulator	Inhibited	−2.003	2.16E−09
HNF4A	Transcription regulator	Inhibited	−2.93	1.33E−04
PKD1	Ion channel	Inhibited	−2	2.34E−02

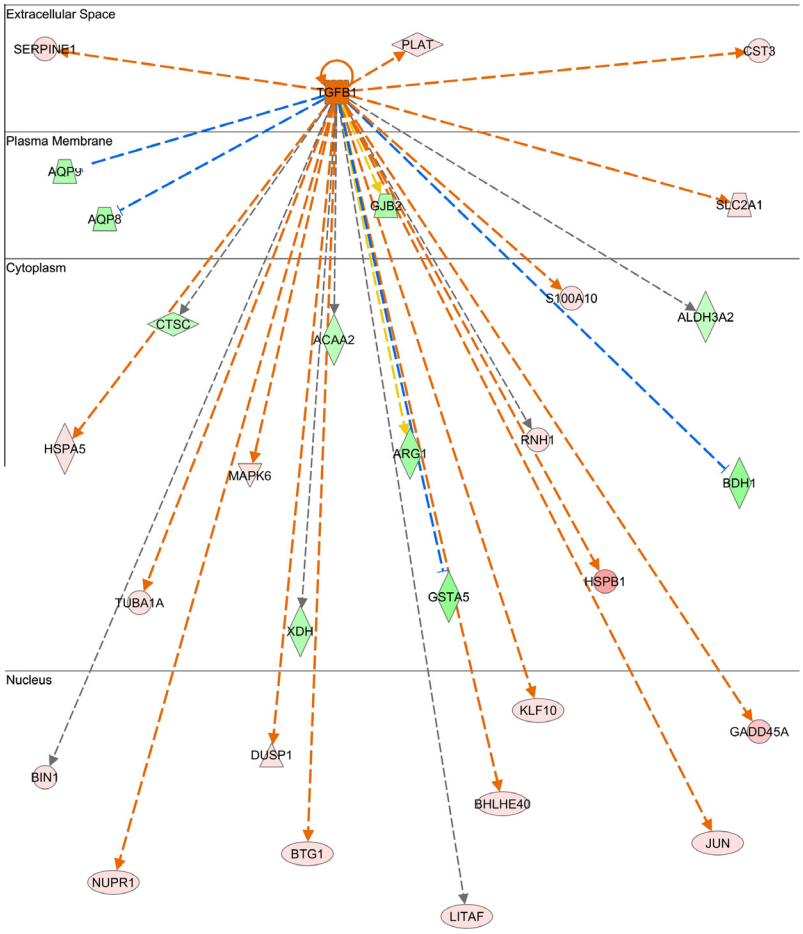

Fig. 4. Upstream regulator TGFB1 and corresponding regulated target genes due to CCl_4 treatment. TGFB1 is predicted as activated and early fibrotic genes such as JUN, MAPK6, PLAT SERPINE1, are causally linked to TGFB1. Their up-regulation due to CCl_4 is consistent with TGFB1 activation. Regulated genes are highlighted in red or green color, based on up or down-regulation respectively; the intensity of the color increases with degree of fold change. The upstream regulator (TGFB1) is indicated as activated (orange) or inhibited (blue) with the color intensity increasing with the confidence level. Orange lines with arrowheads at the end of interactions indicate activation, while blue lines with bars indicate inhibition. Yellow lines indicate inconsistent findings and grey line indicate effect not predicted. (For interpretation of the references to colour in this figure legend, the reader is referred to the web version of this article.)

resulting from regulated genes due to APAP or CCl_4 treatment, it can be seen that, in the case of exposure to CCl_4, genes that have a clear role in fibrosis such as JUN, LITAF, MAPK6, PLAT and SERPINE1 are causally linked to TGFB1 and are up-regulated, but in case of exposure to APAP, only PLAT is up-regulated and causal relation to TGFB1 is seen. It has been reported that TGF-β induces SERPINE1 expression via pSmad2L/C signaling and promotes extracellular matrix deposition in myofibroblasts, thereby accelerating liver fibrosis (Matsuzaki, 2012). This observation indicates a substantial involvement of TGFB1 in the toxicity process initiated by CCl_4 but not by APAP.

Upstream regulator analysis revealed several regulators that control the expression of regulated genes. Predicted activation or inhibition of those regulators and their relation with hepatic fibrosis is outlined here. While a few upstream regulators were activated or inhibited similarly due to APAP and CCl_4 treatment, some regulators were particularly activated or inhibited by either APAP or CCl_4. Toxic concentrations of APAP and CCl_4 are known to induce necrosis in short-term treatment; however, transcriptomic analysis in this study revealed significant differences with respect to genes involved in the toxicity process.

ACOX1, a ROS producing enzyme, is down-regulated due to CCl_4 treatment in our study. A mouse study established the role of ACOX1 in fibrosis showing that ACOX1 knockout mice develop fibrosis (Huang et al., 2011; Ohyama et al., 2012). ACOX1 is down-regulated due to CCl_4 treatment and also 17 genes which have causal relation to it are regulated. In contrast, in the case of exposure to APAP, ACOX1 is not regulated. HNF4A and HNF1A transcription factors are predicted to be inhibited due to both APAP and CCl_4 treatment. HNF4A is involved in differentiation of hepatocytes and is known to be down-regulated in fibrosis (Yue et al., 2010). Furthermore, HNF1A also plays a role in the differentiation of hepatocytes. Therefore, the predicted inhibition of HNF4A and HNF1A due to both APAP- and CCl_4-induced necrosis is possibly related to their general role in the process of differentiation of hepatocytes after induction of necrosis. Inhibition of PPARG and RXRA activity, which is predicted due to CCl_4 treatment but not to APAP, has been shown to lead to hepatic stellate cell proliferation (Sharvit et al., 2013). PPARD agonistic activity leads to anti-fibrotic effects in a fibrosis mouse model induced with CCl_4 (Iwaisako et al., 2012). These results are in accordance with ours, supporting the fibrogenic potential of CCl_4, which is not seen in APAP. PPARA, known to attenuate oxidative stress, one of the most important processes responsible for fibrosis, and to have anti-fibrotic effects in a rat study *in vivo* (Toyama et al., 2004), is predicted to be inhibited by treatment with CCl_4. Thus, the predicted inhibition of PPARA due to CCl_4 also accords with its fibrotic effect. TFAM,

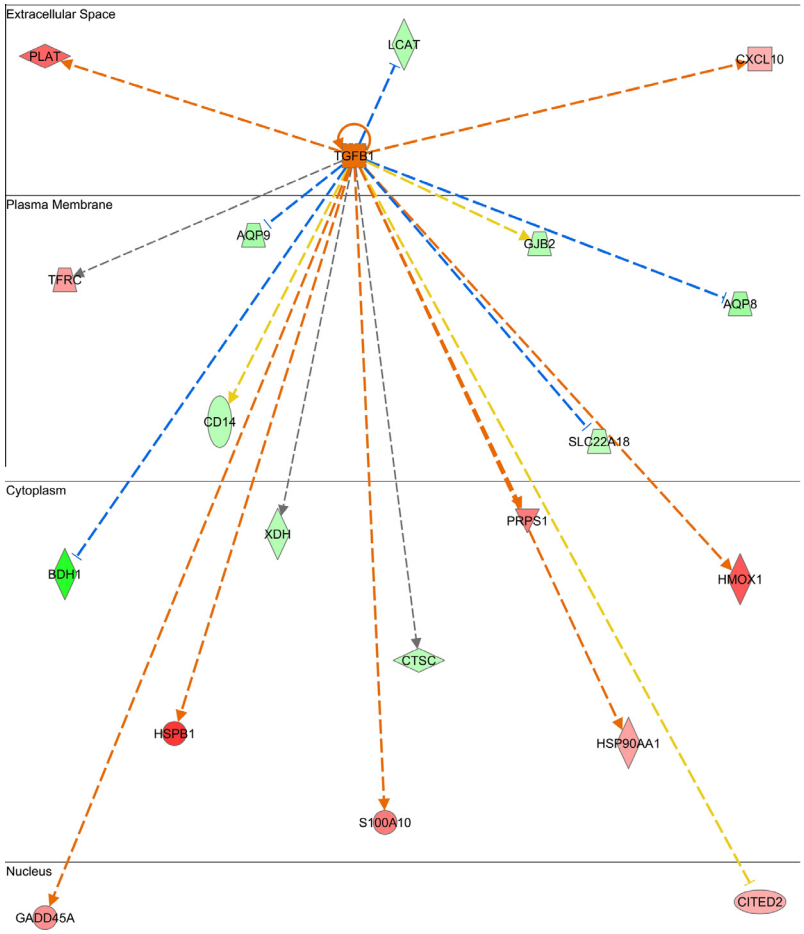

Fig. 5. Upstream regulator TGFB1 and corresponding regulated target genes due to APAP treatment. TGFB1 is predicted as activated but none of the fibrosis related genes are causally linked to TGFB1 except for PLAT. Regulated genes are highlighted in red or green color, based on up or down-regulation respectively; the intensity of the color increases with degree of fold change. The upstream regulator (TGFB1) is indicated as activated (orange) or inhibited (blue) with the color intensity increasing with the confidence level. Orange lines with arrowheads at the end of interactions indicate activation, while blue lines with bars indicate inhibition. Yellow lines indicate inconsistent findings and grey line indicate effect not predicted. (For interpretation of the references to colour in this figure legend, the reader is referred to the web version of this article.)

a mitochondrial transcription factor, is predicted to be inhibited in the case of CCl_4 treatment in PCLS, whereas it was observed to be activated in maintenance of quiescent hepatic stellate cells (Guimarães et al., 2012). No such predicted inhibition of TFAM was seen due to APAP treatment. PKD1, which is predicted to be inhibited in the case of treatment with APAP but not CCl_4, has not been described as playing a potential role in fibrosis up to now. NUPR1, a transcription factor regulating apoptosis is up-regulated due to CCl_4 and was found to be involved in fibrotic changes due to CCl_4 treatment in mice (Ji et al., 2011). ERN1 which is known to play a role in the adaptive response to endoplasmic reticulum (ER) stress is also predicted to be activated due to CCl_4 (Tarrats et al., 2011). In addition, inflammatory cytokines such IL1A, IL1B and TNF are predicted to be activated due to CCl_4. TNF is also known to play a role in HSC proliferation. Overall, transcription factors such as ACOX1, PPARD, PPARA, TFAM, NUPR1, ERN1 and TNF, which are all known to play a role in fibrosis, deregulated, are predicted to be activated or inhibited only due to CCl_4.

Causal network analysis revealed many causal networks which with either one regulator or with groups of interconnected regulators, may have accounted for the observed gene expression changes. Comparison of the causal networks regulated by APAP and CCl_4 revealed interesting differences since many of the networks were specifically found to be activated or inhibited by CCl_4, whereas in the case of APAP few such networks were observed. For instance, causal network containing NOCR2 transcription factor as master-regulator in connection with other intermediate regulators such as AR, ESR1, HNF4A, NCOR2, NR4A1, PGR, PPARG, RXRA, THRB and VDR could account for the observed expression changes of 35 genes regulated due to treatment with CCl_4. TGFB1 was shown to up-regulate NCOR2 expression (Renzoni et al., 2004). A causal network helps to identify novel upstream regulators such as NCOR2 with possible role in hepatic fibrosis, which in-turn helps to derive mechanistic hypothesis. Since the aim of this paper was to explore the differences between APAP and CCl_4 in fibrosis, the causal networks were not explored further in detail.

A recent paper reported the characterization of the proteins involved in hepatic stellate cell activation by CCl_4 *in vitro* (Ji et al., 2012). When we compared the genes regulated in our transcriptomic analysis with the proteins regulated due to CCl_4 treatment in hepatic stellate cells, 17 genes were found in common with the proteins including CRYAB and SERPINE1. Furthermore, a comparison with genes regulated by APAP treatment and proteins involved in HSC activation revealed that 11 are similarly regulated, but none of them overlap with the fibrosis related genes in Table 1 (Supplementary data S3).

In conclusion, in this study we focused on the changes in gene expression profiles due to treatment of PCLS with APAP or CCl_4

and found that those changes reflect the characteristic difference between these compounds in their ability to induce liver fibrosis after chronic dosing *in vivo*. This study indicates that transcriptomic analysis of PCLS can be used to identify the fibrotic potential of toxic compounds after short-term exposure. Further studies with more fibrotic and non-fibrotic compounds are needed to verify this finding and to identify a set of biomarkers that can be used in drug- induced toxicity screening.

Conflict of Interest

The authors declare that there are no conflicts of interest.

Transparency Document

The Transparency document associated with this article can be found in the online version.

Acknowledgments

The authors would like to thank Marja van de Bovenkamp, Annelies L. Draaisma and Marjolijn T. Merema for performing the liver slice experiments. Suzanne Bauerschmidt, Jan Polman and Sjeng J.M.J. Horbach from formerly Schering-Plough for performing hybridization of arrays. The authors also would like to thank ZON MW (3170.0047 & 434023) for financial support.

Appendix A. Supplementary material

Supplementary data associated with this article can be found, in the online version, at http://dx.doi.org/10.1016/j.tiv.2015.03.015.

References

Breitling, R., Armengaud, P., Amtmann, A., Herzyk, P., 2004. Rank products: a simple, yet powerful, new method to detect differentially regulated genes in replicated microarray experiments. FEBS Lett. 573, 83–92. http://dx.doi.org/10.1016/j.febslet.2004.07.055.

Cai, H., Chen, H., Yi, T., Daimon, C.M., Boyle, J.P., Peers, C., Maudsley, S., Martin, B., 2013. VennPlex – a novel Venn diagram program for comparing and visualizing datasets with differentially regulated datapoints. PLoS ONE 8, e53388. http://dx.doi.org/10.1371/journal.pone.0053388.

Ceccarelli, S., Panera, N., De Stefanis, C., Gnani, D., Crudele, A., Rychlicki, C., Petrini, S., Mina, M., Furlanello, C., De Minicis, S., Svegliati-Baroni, G., Nobili, V., Alisi, A., 2014. P280 lps-induced transcription factors involved in non-alcoholic liver disease (nafld) inflammatory and pro-fibrogenic pattern. J. Hepatol. 60, S159. http://dx.doi.org/10.1016/S0168-8278(14)60442-6.

Clouzeau-Girard, H., Guyot, C., Combe, C., Moronvalle-Halley, V., Housset, C., Lamireau, T., Rosenbaum, J., Desmoulière, A., 2006. Effects of bile acids on biliary epithelial cell proliferation and portal fibroblast activation using rat liver slices. Lab. Invest. 86, 275–285. http://dx.doi.org/10.1038/labinvest.3700386.

Dai, Y., Guo, L., Li, M., Chen, Y.-B., 2012. Microarray Я US: a user-friendly graphical interface to Bioconductor tools that enables accurate microarray data analysis and expedites comprehensive functional analysis of microarray results. BMC Res. Notes 5, 282. http://dx.doi.org/10.1186/1756-0500-5-282.

De Graaf, I.A.M., Olinga, P., de Jager, M.H., Merema, M.T., de Kanter, R., van de Kerkhof, E.G., Groothuis, G.M.M., 2010. Preparation and incubation of precision-cut liver and intestinal slices for application in drug metabolism and toxicity studies. Nat. Protoc. 5, 1540–1551. http://dx.doi.org/10.1038/nprot.2010.111.

Eichler, G.S., Huang, S., Ingber, D.E., 2003. Gene Expression Dynamics Inspector (GEDI): for integrative analysis of expression profiles. Bioinformatics 19, 2321–2322.

Ekins, S., 1996. Past, present, and future applications of precision-cut liver slices for *in vitro* xenobiotic metabolism. Drug Metab. Rev. 28, 591–623. http://dx.doi.org/10.3109/03602539608994019.

Elferink, M.G.L., Olinga, P., Draaisma, A.L., Merema, M.T., Faber, K.N., Slooff, M.J.H., Meijer, D.K.F., Groothuis, G.M.M., 2004. LPS-induced downregulation of MRP2 and BSEP in human liver is due to a posttranscriptional process. Am. J. Physiol. Gastrointest. Liver Physiol. 287. http://dx.doi.org/10.1152/ajpgi.00071.2004, G1008-G1016.

Elferink, M.G.L., Olinga, P., Draaisma, A.L., Merema, M.T., Bauerschmidt, S., Polman, J., Schoonen, W.G., Groothuis, G.M.M., 2008. Microarray analysis in rat liver slices correctly predicts *in vivo* hepatotoxicity. Toxicol. Appl. Pharmacol. 229, 300–309.

Ghosh, A.K., Vaughan, D.E., 2012. PAI-1 in tissue fibrosis. J. Cell. Physiol. 227, 493–507. http://dx.doi.org/10.1002/jcp.22783.

Guimarães, E.L., Best, J., Dollé, L., Najimi, M., Sokal, E., van Grunsven, L.A., 2012. Mitochondrial uncouplers inhibit hepatic stellate cell activation. BMC Gastroenterol. 12, 68. http://dx.doi.org/10.1186/1471-230X-12-68.

Guo, C.-J., Pan, Q., Cheng, T., Jiang, B., Chen, G.-Y., Li, D.-G., 2009. Changes in microRNAs associated with hepatic stellate cell activation status identify signaling pathways. FEBS J. 276, 5163–5176. http://dx.doi.org/10.1111/j.1742-4658.2009.07213.x.

Hsiao, Y., Zou, T., Ling, C.-C., Hu, H., Tao, X.-M., Song, H.-Y., 2008. Disruption of tissue-type plasminogen activator gene in mice aggravated liver fibrosis. J. Gastroenterol. Hepatol. 23, e258–e264. http://dx.doi.org/10.1111/j.1440-1746.2007.05100.x.

Huang, J., Viswakarma, N., Yu, S., Jia, Y., Bai, L., Vluggens, A., Cherkaoui-Malki, M., Khan, M., Singh, I., Yang, G., Rao, M.S., Borensztajn, J., Reddy, J.K., 2011. Progressive endoplasmic reticulum stress contributes to hepatocarcinogenesis in fatty acyl-CoA oxidase 1-deficient mice. Am. J. Pathol. 179, 703–713. http://dx.doi.org/10.1016/j.ajpath.2011.04.030.

Iwaisako, K., Haimerl, M., Paik, Y.-H., Taura, K., Kodama, Y., Sirlin, C., Yu, E., Yu, R.T., Downes, M., Evans, R.M., Brenner, D.A., Schnabl, B., 2012. Protection from liver fibrosis by a peroxisome proliferator-activated receptor δ agonist. Proc. Natl. Acad. Sci. USA 109. http://dx.doi.org/10.1073/pnas.1202464109, E1369-76.

Ji, C., Kaplowitz, N., Lau, M.Y., Kao, E., Petrovic, L.M., Lee, A.S., 2011. Liver-specific loss of glucose-regulated protein 78 perturbs the unfolded protein response and exacerbates a spectrum of liver diseases in mice. Hepatology 54, 229–239. http://dx.doi.org/10.1002/hep.24368.

Ji, J., Yu, F., Ji, Q., Li, Z., Wang, K., Zhang, J., Lu, J., Chen, L., E, Q., Zeng, Y., Ji, Y., Qun, E., 2012. Comparative proteomic analysis of rat hepatic stellate cell activation: a comprehensive view and suppressed immune response. Hepatology 56, 332–349. http://dx.doi.org/10.1002/hep.25650.

Jung, D., Elferink, M.G.L., Stellaard, F., Groothuis, G.M.M., 2007. Analysis of bile acid-induced regulation of FXR target genes in human liver slices. Liver Int. 27, 137–144. http://dx.doi.org/10.1111/j.1478-3231.2006.01393.x.

Kluwe, J., Pradere, J.-P., Gwak, G.-Y., Mencin, A., De Minicis, S., Osterreicher, C.H., Colmenero, J., Bataller, R., Schwabe, R.F., 2010. Modulation of hepatic fibrosis by c-Jun-N-terminal kinase inhibition. Gastroenterology 138, 347–359. http://dx.doi.org/10.1053/j.gastro.2009.09.015.

Krämer, A., Green, J., Pollard, J., Tugendreich, S., 2014. Causal analysis approaches in ingenuity pathway analysis. Bioinformatics 30, 523–530. http://dx.doi.org/10.1093/bioinformatics/btt703.

Laskin, D.L., Gardner, C.R., Price, V.F., Jollow, D.J., 1995. Modulation of macrophage functioning abrogates the acute hepatotoxicity of acetaminophen. Hepatology 21, 1045–1050.

Matsuzaki, K., 2012. Smad phosphoisoform signals in acute and chronic liver injury: similarities and differences between epithelial and mesenchymal cells. Cell Tissue Res. 347, 225–243. http://dx.doi.org/10.1007/s00441-011-1178-6.

Ohyama, T., Sato, K., Kishimoto, K., Yamazaki, Y., Horiguchi, N., Ichikawa, T., Kakizaki, S., Takagi, H., Izumi, T., Mori, M., 2012. Azelnidipine is a calcium blocker that attenuates liver fibrosis and may increase antioxidant defence. Br. J. Pharmacol. 165, 1173–1187. http://dx.doi.org/10.1111/j.1476-5381.2011.01599.x.

Olinga, P., Merema, M.T., De Jager, M.H., Derks, F., Melgert, B.N., Moshage, H., Slooff, M.J.H., Meijer, D.K.F., Poelstra, K., Groothuis, G.M.M., 2001. Rat liver slices as a tool to study LPS-induced inflammatory response in the liver. J. Hepatol. 35, 187–194.

Ratziu, V., Lalazar, A., Wong, L., Dang, Q., Collins, C., Shaulian, E., Jensen, S., Friedman, S.L., 1998. Zf9, a Kruppel-like transcription factor up-regulated in vivo during early hepatic fibrosis. Proc. Natl. Acad. Sci. U. S. A. 95, 9500–9505.

Renzoni, E.A., Abraham, D.J., Howat, S., Shi-Wen, X., Sestini, P., Bou-Gharios, G., Wells, A.U., Veeraraghavan, S., Nicholson, A.G., Denton, C.P., Leask, A., Pearson, J.D., Black, C.M., Welsh, K.I., du Bois, R.M., 2004. Gene expression profiling reveals novel TGFbeta targets in adult lung fibroblasts. Respir. Res. 5, 24. http://dx.doi.org/10.1186/1465-9921-5-24.

Rivera, C.A., Bradford, B.U., Hunt, K.J., Adachi, Y., Schrum, L.W., Koop, D.R., Burchardt, E.R., Rippe, R.A., Thurman, R.G., 2001. Attenuation of CCl(4)-induced hepatic fibrosis by GdCl(3) treatment or dietary glycine. Am. J. Physiol. Gastrointest. Liver Physiol. 281, G200–G207.

Rowden, A.K., Norvell, J., Eldridge, D.L., Kirk, M.A., 2006. Acetaminophen poisoning. Clin. Lab. Med.

Schroeder, A., Mueller, O., Stocker, S., Salowsky, R., Leiber, M., Gassmann, M., Lightfoot, S., Menzel, W., Granzow, M., Ragg, T., 2006. The RIN: an RNA integrity number for assigning integrity values to RNA measurements. BMC Mol. Biol. 7, 3.

Sharvit, E., Abramovitch, S., Reif, S., Bruck, R., 2013. Amplified inhibition of stellate cell activation pathways by PPAR-γ, RAR and RXR agonists. PLoS One 8, e76541. http://dx.doi.org/10.1371/journal.pone.0076541.

Smart, D.E., Green, K., Oakley, F., Weitzman, J.B., Yaniv, M., Reynolds, G., Mann, J., Millward-Sadler, H., Mann, D.A., 2006. JunD is a profibrogenic transcription factor regulated by Jun N-terminal kinase-independent phosphorylation. Hepatology 44, 1432–1440. http://dx.doi.org/10.1002/hep.21436.

Takahara, Y., Takahashi, M., Wagatsuma, H., Yokoya, F., Zhang, Q.-W., Yamaguchi, M., Aburatani, H., Kawada, N., 2006. Gene expression profiles of hepatic cell-type specific marker genes in progression of liver fibrosis. World J. Gastroenterol. 12, 6473–6499.

Tarrats, N., Moles, A., Morales, A., García-Ruiz, C., Fernández-Checa, J.C., Marí, M., 2011. Critical role of tumor necrosis factor receptor 1, but not 2, in hepatic

stellate cell proliferation, extracellular matrix remodeling, and liver fibrogenesis. Hepatology 54, 319–327. http://dx.doi.org/10.1002/hep.24388.

Toyama, T., Nakamura, H., Harano, Y., Yamauchi, N., Morita, A., Kirishima, T., Minami, M., Itoh, Y., Okanoue, T., 2004. PPARalpha ligands activate antioxidant enzymes and suppress hepatic fibrosis in rats. Biochem. Biophys. Res. Commun. 324, 697–704. http://dx.doi.org/10.1016/j.bbrc.2004.09.110.

Van de Bovenkamp, M., Groothuis, G.M.M., Draaisma, A.L., Merema, M.T., Bezuijen, J.I., van Gils, M.J., Meijer, D.K.F., Friedman, S.L., Olinga, P., 2005. Precision-cut liver slices as a new model to study toxicity-induced hepatic stellate cell activation in a physiologic milieu. Toxicol. Sci. 85, 632–638.

Westra, I.M., Oosterhuis, D., Groothuis, G.M.M., Olinga, P., 2014a. Precision-cut liver slices as a model for the early onset of liver fibrosis to test antifibrotic drugs. Toxicol. Appl. Pharmacol. 274, 328–338.

Westraa, I., 2014b. The p38-Mapk pathway is involved in fibrogenesis in rat precision-cut liver slices (submitted for publication).

Yue, H.-Y., Yin, C., Hou, J.-L., Zeng, X., Chen, Y.-X., Zhong, W., Hu, P.-F., Deng, X., Tan, Y.-X., Zhang, J.-P., Ning, B.-F., Shi, J., Zhang, X., Wang, H.-Y., Lin, Y., Xie, W.-F., 2010. Hepatocyte nuclear factor 4alpha attenuates hepatic fibrosis in rats. Gut 59, 236–246. http://dx.doi.org/10.1136/gut.2008.174904.